

Symmetry Aspects of H₂ Splitting by Five-Coordinate d⁶ Ruthenium Amides, and Calculations on Acetophenone Hydrogenation, Ruthenium Alkoxide Formation, and Subsequent Hydrogenolysis in a Model *trans*-Ru(H)₂(diamine)(diphosphine) System

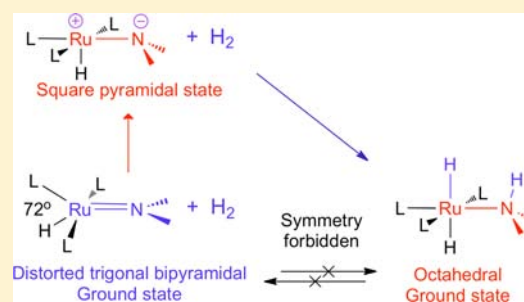
Faraj Hasanayn^{*,†} and Robert H. Morris[‡]

[†]Department of Chemistry, American University of Beirut, Beirut, Lebanon

[‡]Department of Chemistry, University of Toronto, 80 St. George Street, Toronto, Ontario M5S 3H6, Canada

S Supporting Information

ABSTRACT: The potential energy surface (PES) of H₂ addition to the Ru=N bond of a model five-coordinate ruthenium amide (Ru=N), leading to an octahedral *trans*-Ru(H)₂(diamine)(diphosphine) (HRu-NH) and subsequent acetophenone hydrogenation, is studied using M06 density functional theory methods. A qualitative molecular orbital analysis reveals that H₂ addition to the ground state of Ru=N (which has a distorted trigonal-bipyramidal geometry) fits the criterion of a symmetry-forbidden reaction. A transition state (TS) for H₂ heterolytic splitting by Ru=N corresponds to the reaction taking place on an excited state of the Ru=N having a square-pyramidal geometry and gives $\Delta G^{\ddagger} = 19.5$ kcal/mol. The reaction between HRu-NH and acetophenone proceeds by a localized hydride-transfer TS with $\Delta G^{\ddagger} = 11.5$ kcal/mol. This TS leads to an ion pair between a square-pyramidal d⁶ ruthenium amino cation and the alkoxide and is uphill from the separated reactants by 3.5 kcal/mol. Subsequent abstraction of the amino proton by the alkoxide within the ion pair is barrierless, but it also lacks any thermodynamic driving force. In contrast, reorientation of the alkoxide within the ion pair to form an octahedral ruthenium alkoxide is calculated to be exoergic by 7.1 kcal/mol. These features of the PES suggest that the known rapid production of ruthenium alkoxides when stoichiometric amounts of acetophenone and HRu-NH are reacted at low temperatures proceeds by a simple direct route following hydride transfer. For the simplified model complex, ruthenium alkoxide is calculated to be the thermodynamic product of the hydrogenation reaction (exoergic by 3.6 kcal/mol). A TS for H₂ heterolytic splitting across the Ru-alkoxide bond is calculated to have ΔG^{\ddagger} (16.0 kcal/mol), slightly smaller than that of H₂ addition to the five-coordinate Ru=N.

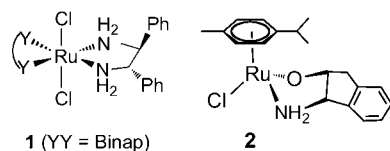


INTRODUCTION

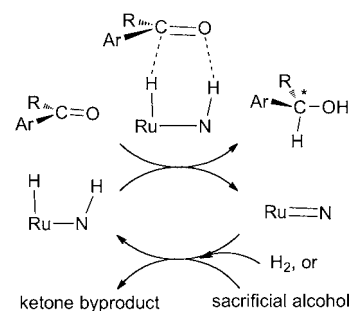
The notion of outer-sphere bifunctional hydrogenation as advocated by Noyori et al. has been instrumental in the development of ruthenium amino complexes that are highly efficient for the selective hydrogenation of ketones^{1,2} and other unsaturated polar bonds such as those of imines and esters.³ The two most prominent families of catalysts of this type are built with the octahedral and piano-stool frames, as illustrated by two examples in Scheme 1.⁴

The general idea of bifunctional hydrogenation is outlined in Scheme 2. Under the conditions used in catalysis, which often

Scheme 1. Examples of Noyori-Type Ketone Hydrogenation Catalysts That Require a Base for Activity



Scheme 2. Idea of Bifunctional Outer-Sphere Ketone Hydrogenation by HRu-NH



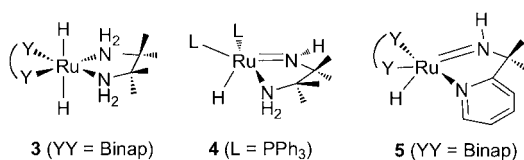
require an alkoxide base, the ruthenium amino complexes are postulated to generate ruthenium amino hydrides (HRu-NH) as active intermediates. The possibility of the formation of a six-membered ring between the HRu-NH (bifunctional) unit and

Received: June 9, 2012

Published: October 2, 2012

the polar unsaturated bond can allow an H^-/H^+ transfer to take place completely in an outer-sphere mode. The resulting ruthenium amide ($Ru=N$) can then react with H_2 or with a sacrificial (transfer) alcohol to regenerate $HRu-NH$. In support of the possibility of this mechanism, the Morris group synthesized examples of octahedral $HRu-NH$ complexes and five-coordinate $Ru=N$ (for example, 3–5 in Scheme 3) that

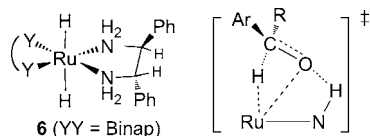
Scheme 3. Isolable Octahedral $HRu-NH$ and Five-Coordinate $Ru=N$ That Catalyze Ketone Hydrogenation without the Need of a Base



could catalyze the hydrogenation of acetophenone using H_2 without the need of an externally added base.^{5–7} A detailed kinetic investigation of acetophenone hydrogenation in benzene using **3** afforded a rate law consistent with a mechanism in which H_2 consumption was rate-limiting in the catalytic cycle.^{6a} Other classes of catalysts that hydrogenate ketones without a base became known later, including a piano-stool $Ru=N$ catalyst for transfer hydrogenation synthesized by Noyori et al.⁸ and a seesaw rhodium amide isolated by Grützmacher et al.⁹

The preparation of solutions of $HRu-NH$ and $Ru=N$ complexes makes it possible to address questions pertaining to the elementary reactions proposed in catalytic cycles. Accordingly, the Bergens group has been conducting low-temperature studies of the reaction of various unsaturated organic substrates with the 1,2-diphenylethylenediamine analogue of **3** (**6** in Scheme 4).

Scheme 4. System Studied by Bergens et al. and a Proposed TS for Carbonyl Group Insertion



Remarkably, a near-quantitative rapid formation of an octahedral ruthenium alkoxide was observed when stoichiometric amounts of acetophenone and **6** were mixed in tetrahydrofuran (THF) at temperatures as low as $-80^\circ C$.^{10,11} Bergens et al. also observed a ruthenium hemiacetaldehyde when **6** was reacted with a lactone.¹² Related octahedral ruthenium alkoxide products were observed by Baratta et al. in the reaction of aromatic ketones with octahedral $[Ru(H)(CNN)(diphosphine)]$ complexes.¹³ Bergens et al. argued that the ruthenium alkoxides could be produced either by stepwise ketone hydrogenation followed by alcohol addition or directly via a transition state (TS) involving partial $Ru-O$ bond formation in the TS between $HRu-NH$ and the ketone, as shown in Scheme 4. The results from trapping experiments designed by the Bergens group to discriminate between the two pathways were supportive of the latter direct route.¹⁴ Interestingly, however, for both **6** and the complexes studied

by Baratta et al., a base was still required for hydrogenation catalysis.

In 2000, Noyori et al. reported a theoretical investigation of the reaction of several unsaturated substrates with a simplified piano-stool $HRu-NH$ as a model of a catalyst like **2**.¹⁵ The calculations verified that outer-sphere hydrogenation is energetically more favorable than the alternative route involving substrate coordination to the metal. The calculated molecular orbitals (MOs) and reaction coordinates (imaginary frequency) in the outer-sphere TSs were consistent with the simultaneous transfer of two hydrogens from the complex to the unsaturated bonds. However, as judged from the atomic charges, Noyori et al. noted in a later study that the extents of the hydridic RuH and protic NH transfers were not completely synchronous.¹⁶ Soon after, in support of experimental studies on ketone hydrogenation by **3**, the Morris group calculated a TS that was presented as connecting the ketone and $HRu-NH$ directly to the final alcohol and $Ru=N$ products.^{6a} Since then, hydrogenation by the $HM-NH$ ($M = \text{metal}$) functionality has been the subject of numerous theoretical investigations conducted in different contexts.^{17–23} Most of these studies report one six-membered TS that is often presented to suggest a synchronous reaction, although the nature of the TS and its reaction coordinates had seldom been discussed. A study by Liu and Lei, however, showed that ketone hydrogenation by octahedral $HRu-NH$ can follow either concerted nonsynchronous or stepwise modes depending on the nature of the ketone.²² Nonetheless, the authors in the latter study appear to assume that each six-membered encounter between a ketone and $HRu-NH$ necessarily leads to the final alcohol and $Ru=N$ products. More recently, in support of experimental studies of new octahedral osmium amino polyhydride catalysts, Gusev and co-workers also calculated sequential hydride- and proton-transfer TSs.²³

An accurate view of the outer-sphere hydrogenation TSs is critical to understanding and developing the chemistry of metal amino hydrides. In the present work, electronic structure methods are used to examine in more detail the nature of elementary reactions in the outer-sphere hydrogenation of acetophenone with the *trans*-ruthenium dihydride system. We first give a qualitative MO analysis that shows that there is an electronic state mismatch between the ground states of the octahedral $HRu-NH$ and its dehydrogenation $Ru=N$ product. To our knowledge, this most fundamental electronic structure aspect of the given bifunctional reaction has not been previously noted although it can have important implications to the H_2 splitting step as well as the ketone hydrogenation step in Scheme 2. An objective of the present work has been to address the question of how the octahedral ruthenium alkoxides may be formed in the given system. The calculated potential energy surface (PES) suggests that this product forms via a hydride-transfer step from $HRu-NH$ to the ketone followed by reorganization of the alkoxide within the intact ion pair. Finally, a calculated TS for hydrogenolysis of the octahedral Ru -alkoxide bond is briefly discussed.

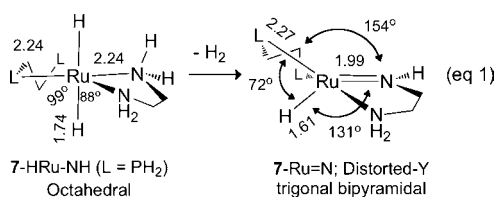
COMPUTATIONAL METHODS

The study has been carried out on a simplified *trans*- $Ru(H)_2(\text{diamine})(\text{diphosphine})$ complex using *Gaussian 09*.²⁴ Only the *trans*-dihydride isomer was considered, implicitly trying to model the reactions of the Binap complexes shown in Scheme 2. Geometry minimization and normal-mode analysis were carried out using M06 density functional theory (DFT)²⁵ in a polarizable continuum model

(PCM)²⁶ with 2-propanol as the solvent. The 6-311G++(2d,2p) basis set was used on the nonmetal elements.²⁷ Ruthenium carried the relativistic effective core potential (ECP) of Hay and Wadt (replacing 28 core electrons)²⁸ and a basis set that included the basis functions supplied with the ECP with the valence functions split into a triple- ζ mode and was augmented with two *f* polarization functions with exponents of 1.24 and 0.4,²⁹ along with one diffuse *d* function with an exponent of 0.015.³⁰ The discussion is based on standard state Gibbs free energies (G°) computed using statistical mechanics methods employing harmonic unscaled vibrational frequencies at 298 K and 1 atm.³¹ We note that the entropy change for associative transformations as obtained by statistical methods is usually exaggerated in favor of the separated parts in comparison with solution reactions, but there is no simple standard solution of the problem.³² All of the important conclusions of the present study are qualitative in nature and are not changed in any way by the entropy factor. We therefore give free energies based on the uncorrected entropies in the figures, and we refer to the effect of the entropy corrections and to other entities such as the standard enthalpies and gas-phase results when they are relevant to the discussion. The different conformations of acetophenone in the complexes were found to differ by less than 2 kcal/mol for a given species. Only the lowest-energy conformers are discussed. The triplet spin state of the five-coordinate Ru=N is calculated to be high in energy and is not discussed.

RESULTS AND DISCUSSION

Symmetry considerations. The model *trans*-Ru(H)₂(diamine)(diphosphine) (7-HRu-NH) used in the calculations and its dehydrogenation Ru=N product (7-Ru=N) are given in eq 1. In this section, we examine in detail the electronic structures of these two species.



7-HRu-NH is an 18-electron complex with an octahedral geometry in which the d^6 electrons occupy a set of nearly degenerate nonbonding (t_{2g}) π -type MOs. The geometry of 7-Ru=N, on the other hand, is distorted trigonal bipyramidal with an amine and a phosphine in the axial positions (at an angle of 173°) and the equatorial groups in a distorted Y

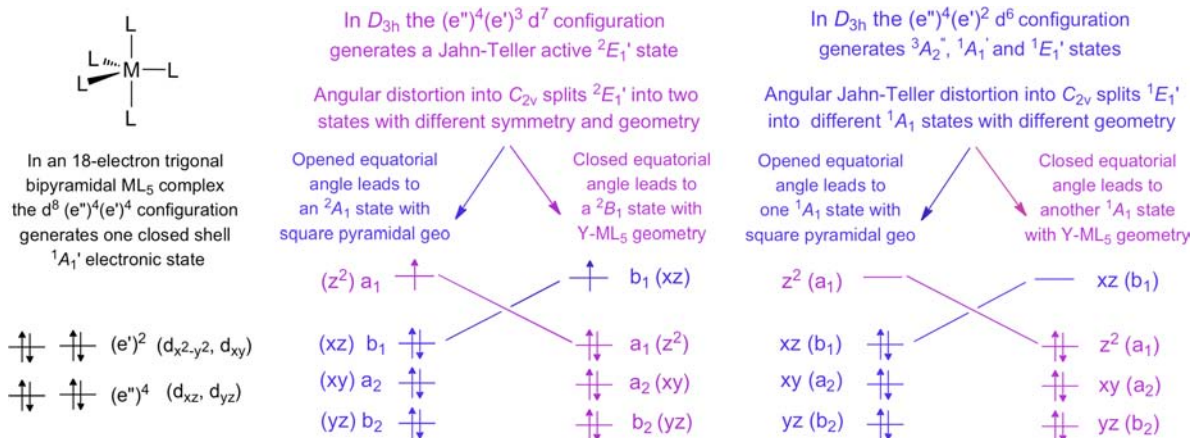
configuration having an angle of 72° between the hydride and a phosphorus of a phosphine. This geometry had been crystallographically determined for both metal amide^{6,7} and nonamide^{33,34} d^6 complexes. A study by Eisenstein et al. provides a theoretical basis to understanding this unconventional geometry,³⁵ but we still find it is helpful to elaborate briefly on the electronic aspects of the problem with the aid of the qualitative MO diagrams of the generic symmetrical d^8 , d^7 , and d^6 ML_5 complexes given in Scheme 5.

In an idealized trigonal-bipyramidal 18-electron ML_5 complex, the d^8 (e'')⁴(e')⁴ configuration generates one closed-shell state (1A_1).³⁶ If an electron is taken out of the valence MO of such a complex, the d^7 (e'')⁴(e')³ configuration would generate a doubly degenerate electronic state ($^2E'$). This state will be subjected to the Jahn–Teller effect, and the D_{3h} geometry generating it will be unstable to distortion.³⁷ Lowering the point group into C_{2v} would split the $^2E'$ state into two nondegenerate 2A_1 and 2B_1 states. One Jahn–Teller distortion mode can take place by opening or closing one of the equatorial angles, and this leads respectively to a square-pyramidal or a distorted trigonal-bipyramidal structure in which the equatorial ligands are in a Y arrangement. The orbital configurations defining the two states will be different in the two geometries (Scheme 4). When the ligands are the same, one geometry will be a minimum and the other a TS connecting two equivalent minima on a Mexican-hat-type PES.^{35,37}

If two electrons were to be removed from the valence MO of the D_{3h} d^8 ML_5 complex, the resulting d^6 (e'')⁴(e')² configuration would generate three electronic states: a triplet $^3A_2'$, an open-shell singlet $^1A_1'$, and a closed-shell $^1E'$. As before, Jahn–Teller distortion into C_{2v} would split the $^1E'$ state into two states distinguished by different d^6 MO occupancies and square-pyramidal or Y geometries. In the square-pyramidal geometry, none of the three MOs containing the d^6 electrons has an a_1 symmetry. In the Y geometry, on the other hand, a pair of d^6 electrons fills an a_1 MO.

When the ligands in the coordination sphere are different, five-coordinate d^6 complexes will still have two low-lying closed-shell states with different geometries and different MO configurations, and their energy order (ground state vs excited state) will depend on the nature of the substituents. The two states can be most conveniently distinguished by the nature of

Scheme 5. MO Occupancies in d^7 and d^6 ML_5 Complexes Differentiating the Electronic States with Square-Pyramidal and Y C_{2v} Geometries



the lowest unoccupied MO (LUMO), which is of the σ -acceptor type in the square-pyramidal geometry and the π -acceptor type in the distorted trigonal-bipyramidal geometry. In the absence of symmetry labels on the MOs, such as in the Ru=NH of interest to the present study, geometry minimization on the closed-shell PES using the single-determinant DFT methods would yield only the ground state of such complexes.³⁸ Nonetheless, the accessibility of the two states and their relevance in bifunctional hydrogenation can be demonstrated without ambiguity by inspecting the MOs in the intermediates obtained by sequential hydride and proton abstraction from 7-HRu-NH (Figure 1).

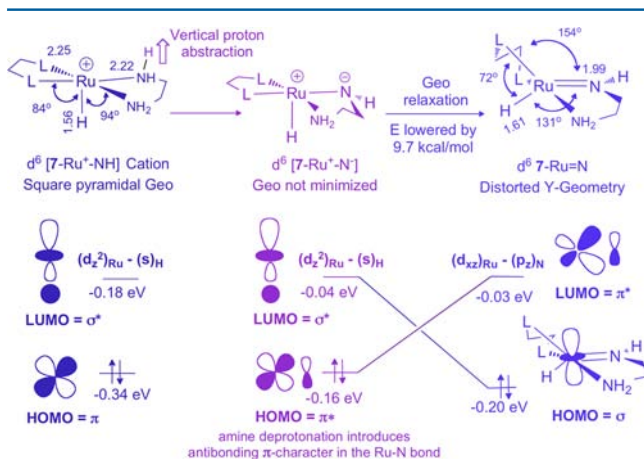


Figure 1. Geometries and MO diagrams for the five-coordinate d^6 [7-Ru⁺-NH] cation and 7-Ru=NH.

Hydride abstraction from 7-HRu-NH followed by geometry minimization gives the 16-electron d^6 [7-Ru⁺-NH] cation with a square-pyramidal ground state as a true minimum on the PES. Although the angular parameters in this cation are similar to the corresponding ones in the parent octahedral 7-HRu-NH, the relaxation energy for the cationic complex obtained by vertical hydride abstraction from 7-HRu-NH to the minimized [7-Ru⁺-NH] is substantial: $\Delta E_{\text{MO6}} = 6.5$ kcal/mol (or 7.8 kcal/mol in the gas phase). This most likely follows from strengthening the Ru-H bond after removal of the hydride from the site trans to it, as can be inferred from a large contraction (from 1.74 to 1.56 Å) in this bond upon geometry relaxation. Related *trans*-hydride effects had been invoked to account for calculated trends in the barriers of alkyl migratory insertion reactions.^{39–41} In comparison, the Ru-N bond distances of [7-Ru⁺-NH] are slightly contracted upon relaxation (by 0.02 Å), whereas the Ru-P bonds are slightly lengthened (by 0.01 Å) during geometry relaxation. In [7-Ru⁺-NH], the d^6 electrons occupy the same set of nonbonding π -type (t_{2g}) metal-based MOs as 7-HRu-NH. With one hydride removed, the LUMO in [7-Ru⁺-NH] is a low-energy σ -type (a_1) MO localized at the vacant coordination site. The strong Ru-H bond brought by placing the hydride at the apical position of the square pyramid is undoubtedly one factor that favors the square-pyramidal state over the Y ML_5 state in the given d^6 cation.

When a proton is subsequently removed from one of the amines of [7-Ru⁺-NH] without geometry minimization to give the square-pyramidal [7-Ru⁺-N⁻] in Figure 1, the symmetry type (σ or π) of the highest occupied MO (HOMO) and LUMO is not changed. However, the HOMO in [7-Ru⁺-N⁻] acquires a small π -antibonding character from interaction

between the metal-based MO and the new filled nonbonding MO of the negatively charged pyramidal amide nitrogen. Figure 1 shows that, upon rearrangement of [7-Ru⁺-N⁻] into the distorted Y geometry of 7-Ru=NH, the d^6 MO configuration is altered such that the LUMO becomes a π -type MO and the HOMO becomes a d_{z^2} σ -type MO. In line with the MO diagrams in Scheme 4 therefore, the given MO and structural differences imply that [7-Ru⁺-N⁻] and 7-Ru=NH have different electronic states. The altered d^6 configuration substitutes a filled–filled π – π interaction between the ruthenium and amide by a filled–empty bonding one in 7-Ru=NH. In other words, changing the electronic state is required to form the Ru–amide π bond, and this can account for the driving force to switch the ground state of the complex when the amine is deprotonated. Consistently, rearrangement from [7-Ru⁺-N⁻] to 7-Ru=NH is accompanied by a large contraction (from 2.22 to 1.99 Å) in the Ru–N bond. We emphasize that the origin of the structural distortions in the given unsaturated system is fundamentally different from the distortions known in five-coordinate 18-electron complexes, where only one electronic state is accessible.

In the gas phase, the relaxation energy (ΔE) from [7-Ru⁺-N⁻] to 7-Ru=NH is calculated to be large: 23.0 kcal/mol. This value should represent an upper limit estimate of the gap between the ground and closed-shell excited states of the Ru=NH. Consistent with the zwitterionic nature of the Ru–amide bond in [7-Ru⁺-N⁻], when the calculations are conducted in a 2-propanol PCM, the gap is reduced to 9.8 kcal/mol. Because the geometries of the two states are related by Jahn–Teller distortions taking place in opposite directions, their energy difference should depend on how all of the Ru–L bonds are changed in the two states. The Ru–amide π bond is only one of these bonds, but it is undoubtedly the critical one that tilts the balance in favor of the distorted trigonal-bipyramidal geometry. All of the isolable five-coordinate complexes with the latter geometry have one π -donor ligand such as an amide, an alkoxide, or a chloride, and the role of ligand-to-metal π donation in stabilizing this geometry had been recognized.^{33,34} The accessibility of two low-energy closed-shell states with different geometries and the role of π -donor ligands in altering their energy order are also applicable in 16-electron piano-stool complexes.^{42,43}

In conclusion to this section, an unsaturated five-coordinate 16-electron complex would have two accessible closed-shell states with geometries related by Jahn–Teller distortion from the idealized trigonal-bipyramidal geometry taking place in two directions. The two states have different numbers of filled σ - and π -type metal-based MOs. The ground state of Ru=NH of interest to the present study has the distorted trigonal-bipyramidal Y geometry, with an empty metal-based π -type MO that is used to make a π bond with the amide. The MO analysis presented in Figure 1 indicates that the ground state of the octahedral 7-HRu-NH (with the d^6 electrons in three π -type MOs) correlates with the excited state of 7-Ru=NH. Because the symmetry (σ vs π) of the three nonbonding metal-based MOs is changed in the reaction, direct hydrogenation reactions involving 7-HRu-NH and 7-Ru=NH should fit the criterion of a symmetry-forbidden reaction.⁴⁴ In light of identifying this electronic condition, we examine in the following sections the nature of the TSs for H₂ splitting and ketone hydrogenation elementary reactions in Scheme 2.

Heterolytic H₂ Making/Splitting. Previous computations showed that H₂ addition/elimination in HRu-NH systems

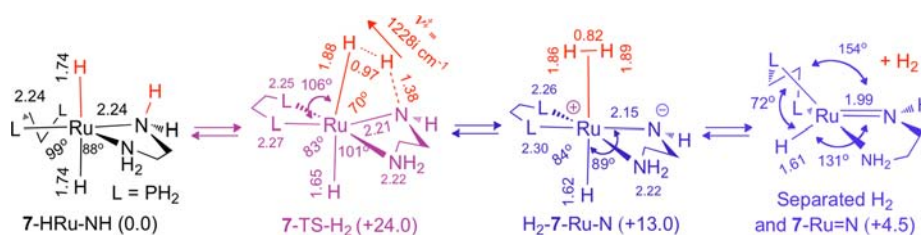


Figure 2. Geometry (in deg and Å) and free energy (G° in kcal/mol) of the TS of heterolytic H_2 making from 7-HRu-NH and the η^2-H_2 intermediate (in 2-propanol as a PCM; L = PH_2). The arrow on 7-TS- H_2 is for the coordinates of ν^\ddagger given in the direction of H–H bond formation.

related to eq 1 involves an η^2-H_2 intermediate and a heterolytic TS.⁶ The structural and energy data of the full species involved in the reaction of the model complex employed in the present study are combined in Figure 2.

The η^2-H_2 -Ru intermediate (H_2 -7-RuN; Figure 2) has a near-idealized octahedral geometry in which the amide moiety is pyramidal and can therefore be viewed as a dihydrogen adduct of the square-pyramidal state of the Ru=N. The Ru–amide bond distance in H_2 -7-RuN (2.15 Å) is significantly shorter than the Ru–amine bond (2.22 Å). As discussed in Figure 1, the Ru–amide π interaction has antibonding character in the square-pyramidal geometry, so the given contraction in the Ru–N bond cannot be a consequence of any Ru–amide π -bonding effects. Instead, the contraction is likely to be a consequence of increased σ donicity of the nitrogen of the pyramidal amide compared to the amine or increased ionic character in the Ru–amide bond. Note that in the η^2-H_2 complex the Ru–P bond distance trans to the amide (2.30 Å) is pronouncedly longer than the Ru–P bond trans to the amine (2.26 Å), which is consistent with a stronger (σ) trans influence from the negatively charged amide compared to the amine in the same complex.

Given that 7-HRu-NH and H_2 -7-RuN are both octahedral and they have the same electronic state of the metal, it follows that the TS connecting them (7-TS- H_2 in Figure 2) should also have the same electronic state. As is clearly indicated by the coordinates of the imaginary frequency (ν^\ddagger ; vector in Figure 2 given in the direction H–H bond making), the TS for heterolytic H–H bond formation is for a localized proton transfer from the NH group of 7-HRu-NH to the Ru–H bond without any concern about electronic effects. The calculated angle between the ruthenium hydride and amide in 7-TS- H_2 is 101° , significantly larger than its value of 89° in either the reactant 7-HRu-NH or the η^2 -adduct product. The opening of this angle in the TS is probably required to bring the amine closer to the hydride to begin heterolytic H_2 making and is by no means an indication of an intermediate value related to a smooth transformation between the octahedral 7-HRu-NH reactant and the final 7-Ru=N product. With 2-propanol as a solvent continuum, the activation barrier (ΔG^\ddagger) from 7-HRu-NH to 7-TS- H_2 is 24.0 kcal/mol, and the reaction energy leading to the η^2-H_2 -Ru adduct is 13.0 kcal/mol. The corresponding energies in the gas phase are 17.3 and 7.4 kcal/mol. Once the uphill η^2-H_2 complex is reached, transformation into free H_2 and 7-Ru=N is thermodynamically favored ($\Delta G^\circ_{\text{diss}} = -8.5$ kcal/mol), driven by the positive entropy of dissociation ($\Delta S^\circ_{\text{diss}} = 29$ eu). We did not address the details of this region of the PES. However, given that the process is an energetically favorable electronic relaxation one, it is highly unlikely for the process to encounter any significant barrier.^{38,45}

By the same arguments as those used to account for H_2 formation from 7-HRu-NH, the ability of 7-Ru=N to split H_2 can be understood to follow from the accessibility of the square-pyramidal state that can bind H_2 . The frontier MOs in the ground state of 7-Ru=N (Figure 1) simply have the wrong symmetry to be able to bind H_2 . The electronic energy of η^2-H_2 -7-RuN is only 1.4 kcal/mol below that of 7-Ru=N ($\Delta E_{\text{coord}} = -1.4$ kcal/mol). The lack of a driving force in this step can be readily attributed to the energy needed to form the square-pyramidal state of the amide, which implicitly involves breaking of the Ru=N π bond before H_2 can coordinate to the metal. As a matter of fact, adding the thermal terms to ΔE_{coord} affords a slightly positive $\Delta H^\circ_{\text{coord}}$ (+0.7 kcal/mol). Adding the entropy terms gives $\Delta G^\circ_{\text{coord}} = +8.5$ kcal/mol (comparable values are obtained in the gas phase). From H_2 -7-RuN, the activation enthalpy of proton transfer from the coordinated H_2 to the nitrogen of the amide to give 7-HRu-NH is 10.0 kcal/mol. This is a surprisingly substantial barrier considering that the reaction is just an intramolecular proton transfer and is thermodynamically favored (by 4.5 kcal/mol). Presumably, the need to reorganize the coordination sphere around the metal to align the incipient amide in the direction of H_2 in the TS adds an important energy input to the activation energy. Combining the two components of the activation process, i.e., excitation of 7-Ru=N and H_2 splitting, gives computed ΔH^\ddagger and ΔS^\ddagger of 10.7 kcal/mol and -29 eu, respectively, relative to the separated H_2 and 7-Ru=N. This leads to $\Delta G^\ddagger = 19.5$ kcal/mol, which although substantial is not prohibitive for facile kinetics. Changing the PCM to benzene has little effect on the calculated barrier. Experimentally, the enthalpy and entropy of activation for catalytic acetophenone hydrogenation by the Binap complex 3 (Scheme 3), as obtained from an Eyring plot of rate constants measured in benzene under constant H_2 pressure in the 283–303 K temperature range, are 8.6 kcal/mol and -27 eu, respectively.^{6a} While admittedly the model complex used in the calculations may be too simplistic to allow for a direct comparison with the Binap complex used in catalysis, as was previously noted,^{6a} the measured barrier for catalysis appears to be smaller than the one calculated based on the TS in Figure 2. A similar conclusion was found in the pyridylamine system (5 in Scheme 3), where the calculated barrier for direct H_2 addition to the Ru=N bond was 19.5 kcal/mol,⁷ but an alcohol-assisted mechanism was calculated to lower the barrier for H_2 splitting to 14.0 kcal/mol (see the subsequent section in the present study).

Reaction of Acetophenone and 7-HRu-NH. The stationary points calculated on the PES of the reaction between acetophenone and 7-HRu-NH are given in Figure 3. By aligning the carbonyl bond of acetophenone in the HRu-NH plane of 7-HRu-NH, we first located a loose precomplex between the two reactants, 7-HRu-Ket. The shortest distance between the two molecules making 7-HRu-Ket is between the

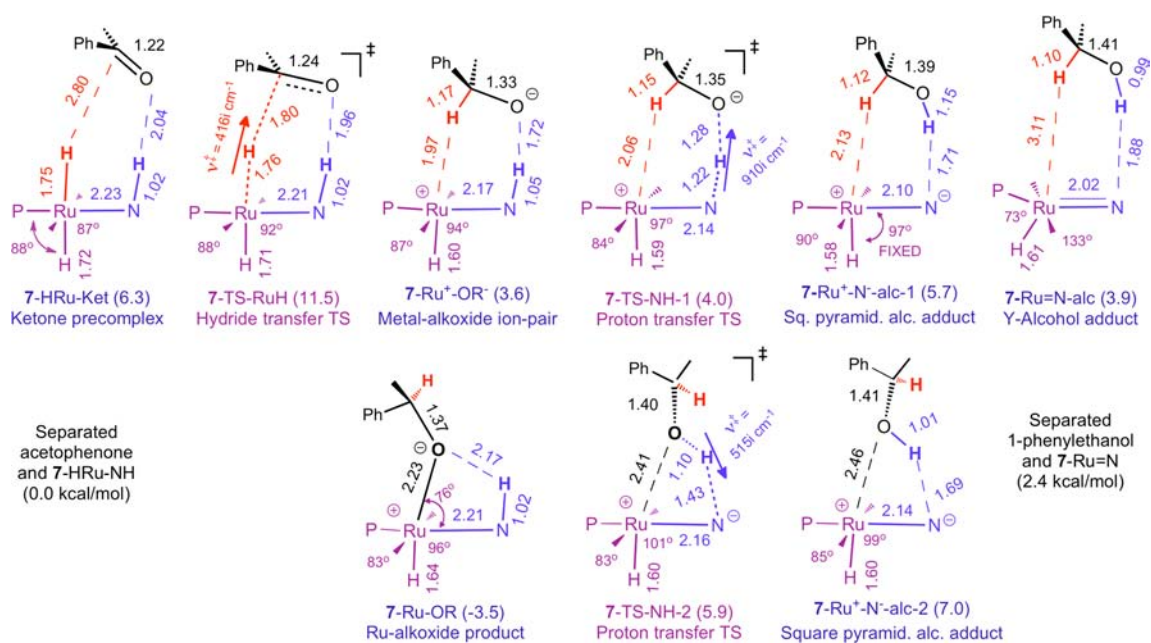


Figure 3. Geometries (in Å and deg) and Gibbs free energies of stationary points on the PES of acetophenone hydrogenation by 7-HRu-NH. The results were calculated in a PCM with 2-propanol as the solvent. Energy values are given relative to the separated reactants (G° at 298 K and 1 atm). The arrows on the TSs are for the coordinates of the corresponding ν^\ddagger given in one direction of the reaction.

oxygen of the ketone and the amino proton: $\text{NH}-\text{O} = 2.04 \text{ \AA}$. This is a relatively long bond and suggests that any hydrogen bonding between the two units is at best weak. The enthalpy and free energy of 7-HRu-Ket relative to the separated reactants are -6.4 and $+6.3$ kcal/mol, respectively. In the gas phase, the relative free energy of 7-HRu-Ket is $+0.6$ kcal/mol. The calculated $\Delta S^\circ_{\text{coord}}$ leading to 7-RuH-Ket is -43 eu. A more realistic estimate of the entropy in solution would probably be closer to -35 eu, which should make the given ΔG° values more exoergic by about 3 kcal/mol at 298 K.

From 7-HRu-Ket, we calculated two TSs and three minima in the direction of the final alcohol product that retain the six-membered ring motif (which is not totally planar in any of the species). In the first TS, 7-TS-RuH, the ketone is brought closer to the HRu-NH moiety such that the bond distance between the incipient carbonyl carbon and the metal hydride becomes shorter than the distance between the amino proton and oxygen ($\text{RuH}-\text{C} = 1.80 \text{ \AA}$ vs $\text{NH}-\text{O} = 1.96 \text{ \AA}$). In the activation process, the $\text{Ru}-\text{H}$ and $\text{N}-\text{H}$ (1.76 and 1.02 Å) bond distances are barely changed from their respective equilibrium values in the precomplex (1.75 and 1.02 Å). Nonetheless, 7-TS-RuH has one imaginary frequency ($\nu^\ddagger = 416i \text{ cm}^{-1}$) that is unambiguously characteristic of the pure motion of the hydride between the ruthenium and carbonyl carbon centers (shown as a vector in the direction of $\text{Ru}-\text{H}$ dissociation in Figure 3). For the given model reaction, the activation enthalpy from separated reactants to 7-TS-RuH is calculated to be slightly negative ($\Delta H^{\circ\ddagger} = -3.5$ kcal/mol), implying a diffusion-controlled reaction.

In accordance with a hydride-transfer step taking place independently from proton transfer, we minimized 7-Ru⁺-OR⁻ in Figure 2, an ion pair between the square-pyramidal [7-Ru⁺-NH] cation (Figure 1) and the alkoxide with the newly formed C-H bond still pointed toward the ruthenium atom. The distance between the newly formed C-H bond and the metal is 1.97 Å, which is not particularly indicative of significant CH-Ru bonding. Not surprisingly, on the other hand, the distance

between the now negatively charged oxygen and the amino proton in 7-Ru⁺-OR⁻ is short ($\text{NH}-\text{O} = 1.72 \text{ \AA}$), reflecting a strong hydrogen bond between the two units. In spite of the charge-separation nature of the transformation, the reaction free energy from the separated ketone and 7-HRu-NH to 7-Ru⁺-OR⁻ is enthalpically favorable ($\Delta H^\circ = -11.2$ kcal/mol) and is only slightly exoergic ($+3.6$ kcal/mol).

With the $\text{NH}-\text{O}$ hydrogen bond in place, proton transfer from the amine to the coordinated alkoxide within 7-Ru⁺-OR⁻ proceeds via 7-TS-NH for a localized motion of the proton between the nitrogen and oxygen atoms ($\nu^\ddagger = 910i \text{ cm}^{-1}$; Figure 3). The electronic energy (E_{M06}) of 7-TS-NH is 2.9 kcal/mol above 7-Ru⁺-OR⁻. When the terms of the free energy are added, 7-TS-NH becomes 0.4 kcal/mol above the 7-Ru⁺-OR⁻ ion pair. The coordination sphere around the metal in this TS is largely square-pyramidal. This means that proton transfer, and thereby the full outer-sphere ketone hydrogenation process, takes place entirely on the same PES of the initial octahedral dihydride. As such, proton transfer is likely to give at first an intermediate corresponding to an adduct between the square-pyramidal state of the amide and the alcohol reminiscent of the $\eta^2\text{-H}_2$ adduct discussed in Figure 2. However, attempts to minimize the geometry of such species encountered problems in the convergence of the displacements of the coordinates (but not in the forces) that were dependent upon the basis set, gas, or PCM and the quality of the force constant matrix used in the minimization. To circumvent this problem and to allow for consistency and reproducibility, we conducted geometry minimization starting with the parameters of 7-TS-NH but with the $\text{H}-\text{Ru}-\text{N}$ angle fixed at its value in the TS (97°). The results afforded 7-Ru⁺-N⁻-alc-1 in Figure 3, which is fully consistent with an alcohol adduct of the square-pyramidal state of the $\text{Ru}=\text{N}$ that is stabilized by a hydrogen bond between the alcoholic proton and the negatively charged amide ($\text{O}-\text{H} = 1.15 \text{ \AA}$ and $\text{OH}-\text{N} = 1.71 \text{ \AA}$). Specifically, in 7-Ru⁺-N⁻-alc-1, the $\text{H}-\text{Ru}-\text{P}$ angle is 90° and the amide moiety is pyramidal. The distance between the alcoholic proton and the amide center is

short in this adduct ($\text{OH-N} = 1.71 \text{ \AA}$). The electronic energy (E_{M06}) of $7\text{-Ru}^+\text{-N}^-\text{-alc-1}$ is 1.1 kcal/mol below $7\text{-Ru}^+\text{-OR}^-$. Although the given adduct is minimized with one frozen parameter, normal-mode analysis (no imaginary frequencies), and the force constant matrix it generated (no negative eigenvalues, along with a satisfactory force constant and coordinate displacement convergences), both characterize it as a true minimum on the PES. The free energy obtained from the latter calculations puts the adduct at 2.1 kcal/mol above $7\text{-Ru}^+\text{-OR}^-$ (with PCM). In the gas phase, $7\text{-Ru}^+\text{-N}^-\text{-alc-1}$ is 1.6 kcal/mol below the ion pair (on the G° scale).

The last six-membered species in Figure 3 is $7\text{-Ru}=\text{N-alc}$. Here the moiety around the amido nitrogen is planar, the Ru–N bond is short (2.02 Å), the N–Ru–H angle is wide (133°), and the H–Ru–P angle is narrow (73°), all characteristic of the ground state of $\text{Ru}=\text{N}$. In this adduct, the distance between the alcoholic proton and the amide nitrogen is long ($\text{OH-N} = 1.95 \text{ \AA}$). $7\text{-Ru}=\text{N-alc}$ is 1.8 kcal/mol more stable than $7\text{-Ru}^+\text{-N}^-\text{-alc-1}$ (it is this slightly lower energy that complicates full geometry minimization of $7\text{-Ru}^+\text{-N}^-\text{-alc-1}$).⁴⁶ The comparable energy of the very different alcohol adducts obviously follows from very different effects: an additional Ru–amide π bond in the Y state against strong hydrogen bonding between the alcohol and negatively charged amide center in the square-pyramidal state. Noteworthy, the Ru–H bond in $7\text{-Ru}^+\text{-N}^-\text{-alc-1}$ is 1.58 Å, significantly shorter than that in the Y adduct (1.61 Å). The strengthening of the Ru–H bond in $7\text{-Ru}^+\text{-N}^-\text{-alc-1}$ is one factor that favors the square-pyramidal state of $\text{Ru}=\text{N}$. As was the case with the $\eta^2\text{-H}_2$ complex, $7\text{-Ru}^+\text{-N}^-\text{-alc-1}$ is unstable to dissociation into separated 1-phenylethanol and $7\text{-Ru}=\text{N}$ but by only 3.2 kcal/mol. The calculated free-energy change from separated reactants to the separated alcohol and $7\text{-Ru}=\text{N}$ is +2.4 kcal/mol (in PCM). In contrast, in the gas phase, the process is exoergic (–4.3 kcal/mol).

In addition to the two six-membered alcohol adducts, we calculated another adduct of the square-pyramidal state of $\text{Ru}=\text{N}$ in which the alcoholic O–H bond makes a four-membered ring with the Ru–amide bond ($7\text{-Ru}^+\text{-N}^-\text{-alc-2}$; Figure 3). Although the alcoholic oxygen in $7\text{-Ru}^+\text{-N}^-\text{-alc-2}$ is in close proximity to the metal center, the Ru–O bond distance of 2.46 Å is too long to implicate any significant covalent bonding between the oxygen and the empty coordination site on the metal. Thus, the stability of this adduct appears to be driven by a dipole–dipole attraction between the O–H and zwitterionic Ru–amide bonds. As such, $7\text{-Ru}^+\text{-N}^-\text{-alc-1}$ and $7\text{-Ru}^+\text{-N}^-\text{-alc-2}$ can be viewed as conformers related by rotation of the alkyl group of the alcohol (along the C–O bond while maintaining an OH–N hydrogen bond). In the gas phase, the two adducts are calculated to have nearly identical energy, whereas in the 2-propanol PCM, the six-membered conformer is more stable by 1.3 kcal/mol.

From $7\text{-Ru}^+\text{-N}^-\text{-alc-2}$, a barrierless four-membered TS for proton “retransfer” from the alcohol to the amide leads to a ruthenium alkoxide complex, 7-Ru-OR . Interestingly, the alkoxy group in 7-Ru-OR is significantly bent toward the amine, making an O–Ru–N angle of 76° , and the Ru–O bond distance is relatively long at 2.23 Å. In the 1-phenylethanol complex of the Ru–Binap complex **2** in Scheme 2, the Ru–OR bond distance is 2.32 Å and the tilting angle is 74° .⁴⁷ Related bending and long Ru–OR distances had been crystallographically determined for an octahedral *trans*-hydridoruthenium phenoxide complex obtained from phenol addition to $\text{Ru}=\text{N}$ **4** in Scheme 1, with an additional phenol molecule

hydrogen bonding with the oxygen of the coordinated phenoxide.⁴⁸ Such bending may be driven to introduce a long-range hydrogen bond between the oxygen and the amino proton, although the NH–O bond distance (2.08 Å) seems too long to implicate a strong hydrogen bond. As a matter of fact, tilting has been observed in the crystal structure of *trans*- $[\text{Ru}(\text{H})(\text{OC}_6\text{H}_4\text{-p-Me})(\text{dmpe})_2]$, where hydrogen bonding to an amine is not applicable.⁴⁹ Given the strong *trans* influence of the hydride, the covalent character in the Ru–O bond is expected to be weak in the octahedral motif, so the energy needed to bend the O–Ru–N angle should not be large, and it may even lead to strengthening of the Ru–H bond (which has a bond distance of 1.64 Å in 7-Ru-OR). In spite of the tilting, 7-Ru-OR is calculated to be the lowest-energy species in Figure 2, with a standard state free energy of –3.5 kcal/mol relative to the separated acetophenone and 7-HRu-NH or –6.0 kcal/mol relative to the separated 1-phenylethanol and $7\text{-Ru}=\text{N}$ (in PCM). In the gas phase, the thermodynamic stability of 7-Ru-OR is much larger: –12.3 kcal/mol relative to separated acetophenone and 7-HRu-NH or –8.0 kcal/mol relative to $7\text{-Ru}=\text{N}$ and the alcohol.

Mechanism of Ruthenium Alkoxide Formation. The PES in Figure 3 implicates $7\text{-Ru}^+\text{-OR}^-$ as an ion-pair intermediate following hydride transfer from 7-HRu-NH to acetophenone. From the ion pair, proton transfer to produce either the coordinated or separated alcohol products lacks any thermodynamic driving force, with the energies of the six-membered species all varying within less than 2 kcal/mol. In contrast, the transformation from $7\text{-Ru}^+\text{-OR}^-$ to the octahedral ruthenium alkoxide is exoergic by 7.1 kcal/mol (or by 12.2 kcal/mol in the gas phase). Although the oxygen of the alkoxide in the six-membered motif of $7\text{-Ru}^+\text{-OR}^-$ may be in the right position to immediately abstract a proton from the amine, all that is needed to begin making the Ru–OR bond from $7\text{-Ru}^+\text{-OR}^-$ is a simple reorientation of the alkoxide so that the oxygen points in the direction of the metal. Close inspection of the geometry of $7\text{-Ru}^+\text{-OR}^-$ does not reveal any structural features that may obstruct such a reorientation, so the rearrangement is unlikely to encounter any significant kinetic barrier. Indeed, a one-dimensional PES scan defined by a gradual opening of the O–Ru–N angle from its value of 48° in the ion pair to 74° in 7-Ru-OR shows an initial gradual increase in the electronic energy (ΔE_{M06}), reaching a maximum of only 1.8 kcal/mol above the $7\text{-Ru}^+\text{-OR}^-$ minimum before the energy drops sharply toward 7-Ru-OR . The 1.8 kcal/mol barrier on this pathway is smaller than the value for $\Delta E_{\text{M06}}^\ddagger$ (2.9 kcal/mol) for proton transfer from the amino nitrogen to the alkoxide (via 7-TS-NH-1). Under these conditions, the precise behavior of the system past hydride transfer is likely to be governed by dynamics details. Given the flat nature of the PES in the direction of proton transfer from the amine, it will be highly improbable that the simple rotation required to realign the alkoxide could completely shut down its rapid formation following hydride transfer. The calculation of a kinetically facile distinct hydride-transfer step from 7-HRu-NH to the ketone can therefore provide a simple explanation for the low-temperature formation of ruthenium alkoxides. Baratta et al. used related arguments to rationalize metal alkoxide formation in the reaction between ketones and $[\text{Ru}(\text{H})(\text{CNN})(\text{diphosphine})]$ complexes.⁵⁰ Note that the net reaction from separated ketone and 7-HRu-NH to 7-Ru-OR is a carbonyl group insertion into an M–H bond taking place without initial coordination of the ketone. The reverse of this unconventional insertion is β -

hydride elimination from the alkoxide in the octahedral 7-Ru-OR taking place without utility of a cis empty coordination site. Such unconventional β -hydride elimination has precedence in both octahedral⁵¹ and piano-stool⁵² systems, although the proposed mechanisms have varied. Recently, Milstein et al. observed β -hydride elimination from an octahedral ruthenium alkoxide taking place at $-30\text{ }^{\circ}\text{C}$.⁵³

In conclusion to this section, the observed low-temperature formation of ruthenium alkoxide in the reaction between ketones and *trans*-dihydride complexes can be viewed as a direct insertion reaction of the carbonyl group of the ketone into a metal hydride bond taking place via hydride transfer and ion-pair rearrangement.

Hydrogenolysis of Ruthenium Alkoxide. The calculated ΔG° for the formation of 7-Ru-OR by acetophenone insertion in the model 7-HRu-NH complex is -3.0 kcal/mol . Experimentally, the addition of 1 equiv of acetophenone to THF solutions of $\text{Ru}(\text{H})_2(\text{Binap})(1,2\text{-diphenylethylenediamine})$ (**6** in Scheme 4) leads to the rapid formation of ruthenium alkoxide.¹¹ In contrast, this product is not observed in the corresponding reaction of the analogous tetramethylenediamine complex (**3** in Scheme 2) in benzene at room temperature.^{6a} Under catalytic conditions (benzene, room temperature), the latter reaction produces 1-phenylethanol in equilibrium with the five-coordinate $\text{Ru}=\text{N}$.^{6a} As mentioned in the Introduction, while **3** catalyzes hydrogenation without an external base, **6** requires a base for catalytic activity. These observations demonstrate a delicate balance in the energy of the different species considered in Figure 2 and show that they are highly sensitive to the substituents on the diamine ligand. Given that the model complex employed in the present study omits the substituents from the diamine altogether and uses a simplistic diphosphine in place of Binap, the present study is obviously not in a position to make statements regarding the reactivity of ruthenium alkoxides and their possible role in catalysis. However, in the past Noyori et al. had raised the possibility of alcohol and base-assisted H_2 cleavage mechanisms in order to account for the observation that external bases and protic solvents tend (but not always) to speed the rates of ketone hydrogenation with H_2 .^{7,54,55} Casey et al. also invoked a solvent-assisted H_2 splitting in hydrogenation with Shvo-type catalysts.⁵⁶ An NMR study by Schneider et al. gave support for such a mechanism with a water molecule as the assisting group.⁵⁷ The calculated solvent-assisted H_2 -splitting TSs have often been presented to represent proton transfer from H_2 to the alcohol taking place concomitantly with proton transfer from the alcohol to $\text{Ru}=\text{N}$ (relay or shuttle mode).^{7,21d,58,59} Given the focus of the present study on the detailed nature of the TSs commonly invoked in hydrogenation catalysis, we became interested in analyzing more closely the solvent-assisted H_2 TSs. Surprisingly, we could not identify a TS that would satisfy the commonly presented relay solvent-assisted description. Instead, we calculated 7-TS- H_2 -OR in Figure 4, characterized by a short H–H bond (0.88 Å, compared to 0.97 Å in 7-TS- H_2 ; Figure 2) and a short distance between H_2 and the oxygen of the organic substrate (HH–O = 1.47 Å). Significantly, the distance between the amino proton and the oxygen atom is long in this TS (NH–O = 1.84 Å).

The imaginary frequency in 7-TS- H_2 -OR has a large component for motion of the protic hydrogen of H_2 , along with a smaller yet significant component from the hydridic end, both moving in the same direction as shown by the two arrows on this TS in Figure 4. No contribution from the proton of the

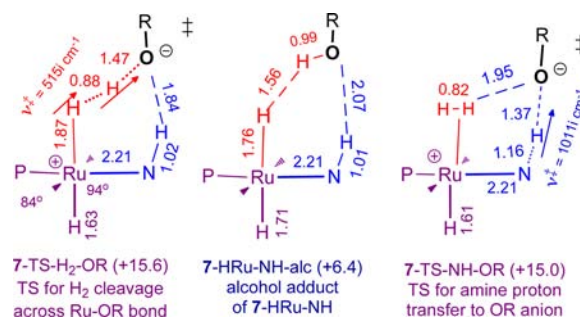


Figure 4. Geometries (in Å and deg) and Gibbs free energies for H_2 cleavage by 7-Ru-OR (R = 1-phenylethyl). The results were calculated in a PCM with 2-propanol as the solvent. Energies are given relative to the separated H_2 and 7-Ru-OR (G° at 298 K and 1 atm).

amine appears in the reaction coordinate. 7-TS- H_2 -OR is therefore consistent with a H_2 molecule being split by an alkoxide and the square-pyramidal ruthenium amino cation. The participation of the two hydrogen atoms in the reaction coordinate in this TS is in striking contrast with H_2 splitting across the $\text{Ru}=\text{N}$ bond in Figure 2, where the imaginary frequency is for a purely localized proton transfer taking place between the HRu-NH and $\text{Ru}=\text{N}$ centers. In accordance with fundamentally different reaction coordinates, the values of the imaginary frequencies are very different in the two TSs: 515 i cm^{-1} in 7-TS- H_2 -OR (Figure 4) against 1228 i cm^{-1} in 7-TS- H_2 (Figure 2). These results are suggestive of some degree of concertedness in the H_2 splitting mode across the Ru–OR bond. Because 7-Ru-OR is calculated to be the thermodynamic product in Figure 3, 7-TS- H_2 -OR may be viewed as a direct H_2 addition across the Ru–OR bond. A concerted σ -bond metathesis mode of H_2 splitting had been implicated in hydrogenolysis of the M–C bonds of early-transition-metal complexes where the M–C bond may also have significant ionic character.⁶⁰ More importantly, Goldberg and co-workers provided kinetics and computational evidence in support of σ -bond metathesis in hydrogenolysis of square-planar palladium alkoxides, leading directly to alcohols and square-planar palladium hydrides.⁶¹ Noteworthy, Yang calculated H_2 cleavage across an Fe–OR bond in the cycle of acetophenone hydrogenation by an Fe-PNP system lacking the amide/amine functionality,⁶² but the reaction was depicted as an attack of a free alkoxide (generated in the course of the hydrogenation cycle and then dissociated from an octahedral Fe-OR complex) to a cationic octahedral $\eta^2\text{-H}_2$ complex. Regardless of the details by which 7-TS- H_2 -OR is reached, the free-energy difference from separated H_2 and 7-Ru-OR to 7-TS- H_2 -alc is 15.6 kcal/mol, significantly *smaller* than the barrier of 19.5 kcal/mol calculated for H_2 addition to 7-Ru= N (Figure 2). This is in line with the findings presented as solvent-assisted H_2 splitting. Interestingly, the alcohol adduct resulting from H_2 cleavage in Figure 4 (7-HRu-NH-alc) is 6.4 kcal/mol above the separated H_2 and 7-Ru-OR and is unstable to alcohol dissociation by 5.0 kcal/mol. The calculated production of 7-HRu-NH and an alcohol from 7-Ru-OR and H_2 is endoergic by 1.4 kcal/mol. In contrast, H_2 addition to 7-Ru= N was exoergic by 4.5 kcal/mol. In other words, the calculations predict H_2 addition to the Ru–OR bond to be kinetically faster than addition to $\text{Ru}=\text{N}$ but thermodynamically less favorable. In the Pd-OR system, the barrier of H_2 addition was at 25 kcal/mol.⁶¹ The calculated low barrier in 7-Ru-OR is probably a result of the looseness of the Ru–alkoxide bond in 7-Ru-OR (Figure 3).

Although we are not aware of conclusive experiments that H₂ addition to analogues of 7-Ru-OR can be kinetically more favorable than H₂ addition to 7-Ru=N, consideration of the reverse reaction shows that this prediction is not unreasonable. Specifically, Bergens et al. observed that the addition of certain alcohols to the octahedral Ru-Binap dihydride in Scheme 4 at $-80\text{ }^{\circ}\text{C}$ (without added base) leads to the rapid formation of H₂ and ruthenium alkoxides. Bergens et al. considered only one possibility for the mechanism of this reaction involving H₂ heterolytic dissociation to give Ru=N and a subsequent bifunctional alcohol addition to the Ru=N bond. According to our model calculations, the barrier to H₂ elimination would be 24 kcal/mol, indicating a slow H₂ dissociation at $-80\text{ }^{\circ}\text{C}$. On the other hand, the calculations predict the direct (associative) reduction of the alcohol via 7-TS-H₂-OR to have $\Delta G^{\ddagger} = 14.1$ kcal/mol (based on a calculated associative entropy of activation of -42 eu). The *trans*-Ru(H)₂ complex studied by Bergens et al. is established to be a powerful hydride donor, thus reducing ketones (directly into Ru-OR)¹⁴ and even esters (directly into ruthenium hemiacetaloxides)¹² rapidly at $-80\text{ }^{\circ}\text{C}$. Our calculations of hydride transfer to acetophenone predict a negative enthalpy of activation. It is not unreasonable therefore for the same mechanism to be operative in the observed reaction between the *trans*-Ru(H)₂ and H-OR bonds. Such a mechanism will be similar to that of alcohol reduction by alkali hydrides. Clearly, it will be of interest to test the computed predictions experimentally. Given that one pathway for alcohol reduction by *trans*-Ru(H)₂ complexes is dissociative while the other is associative, a straightforward study of the kinetics of this reaction (occurring at the minute scale at $-80\text{ }^{\circ}\text{C}$ for some alcohols in the Bergens system)¹⁴ should discriminate between the two mechanisms, and this should test the unexpected prediction that hydrogenolysis of Ru-OR can be kinetically faster than H₂ addition to Ru=N. We emphasize that our results as obtained for a model system may not extend uniformly to the different Binap systems and different alcohols. The energetics of the given reaction will depend on the pK_a of the alcohol and strength of the Ru-alkoxide bond, which can vary significantly from system to system.

As a further support of the above interpretation of 7-TS-H₂-OR, we calculated another TS corresponding to pure proton transfer from the amino group of the cationic (octahedral) η^2 -H₂ adduct to the alkoxide (7-TS-NH-OR in Figure 4). Remarkably, this TS is predicted to have an energy nearly identical with that of H₂ addition to Ru-OR. Thus, the variations in the nature of the alcohol or base-assisted TSs as reported in different computational studies can be a consequence of the details of the acidity of the coordinated H₂, amine, and alcohol (for example, 1-phenylethanol vs methanol) and may vary depending on the theoretical model and level of theory used in the calculations. Addressing the importance of these factors in a systematic way is beyond the scope of the present study.

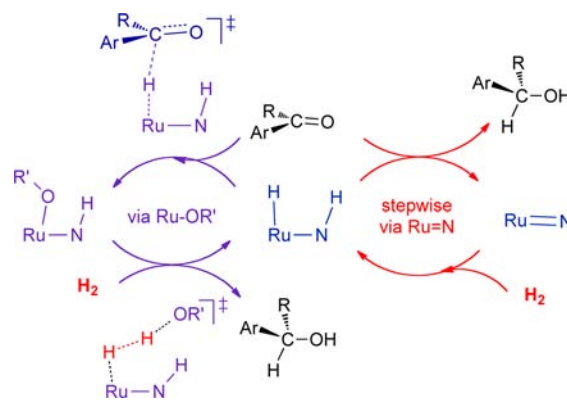
CONCLUSIONS

The catalytic cycles of ketone hydrogenation by HRu-NH have been the subject of experimental and theoretical investigations before. The present computational work revisits this system and identifies new electronic, structural, and energetic features of the TSs and minima on the PES that are fundamental to understanding the chemistry of these catalysts. First, an MO analysis demonstrates that interconversion between the ground states of the HRu-NH and its dehydrogenation Ru=N product

is symmetry-forbidden. The ability of the five-coordinate d⁶ Ru=N to cleave H₂ heterolytically follows from the accessibility of a low-energy excited state of Ru=N having a square-pyramidal geometry. For acetophenone hydrogenation by 7-HRu-NH, the study provides evidence for an outer-sphere sequential hydride- and proton-transfer reaction mode taking place on the square-pyramidal state of the amide and not a synchronous one. As standard state conditions, the thermodynamic product of the given reaction is calculated to be octahedral ruthenium alkoxide, corresponding to insertion of the carbonyl of acetophenone in a Ru-H bond. This reaction is the reverse of β -hydride elimination from a metal-alkoxide bond of an 18-electron complex, which has precedence. We propose that a simple rearrangement of the alkoxide within the ion pair following hydride transfer may account for the mechanism of low-temperature observation of ruthenium alkoxides in the reaction of acetophenone and *trans*-ruthenium dihydride complexes. Finally, a TS for H₂ addition to 7-Ru-OR affords an activation barrier for H₂ splitting that is slightly smaller than the barrier for direct H₂ addition to the Ru=N bond of five-coordinate Ru=N.

Taken at face value, the collective results from the new calculations can be used to add a branch to the commonly used amide-based scheme of ketone hydrogenation (Scheme 6).

Scheme 6. Two Possible Branches for Ketone Hydrogenation



Given the prevalence of ion pairs and proton- and hydride-transfer reactions in the two branches, the energetics and contribution of the two cycles in catalysis will depend on the concentration of the species involved, the acidity of the alcohol and the amine ligand, and the solvation (bulk, coordination, and hydrogen-bonding) effects.⁴⁸ For example, some alcohols are known to react with *trans*-Ru-Binap dihydride complexes (giving ruthenium alkoxide and H₂), while others do not.¹⁴ In catalysis, an isolable octahedral ruthenium phenoxide complex is not active,⁴⁸ whereas octahedral ruthenium isopropoxides studied by Bergens et al. are active only when a base is added.¹¹ Similarly, Baratta et al. gave evidence that ruthenium alkoxides can be active in catalytic transfer hydrogenation, although, again, a base was also required in these systems.^{13,50} Such effects are hard to describe accurately by conventional computational methods on model complexes such as the ones employed in our study. This was demonstrated, for example, in a quantum-chemical dynamics study by Meijer and Haandgraf (yet, necessarily, using model complexes and methanol as the solvent), which showed that solvent PCMs can have limitations in bifunctional hydrogenation reactions.⁶³

However, from a computational perspective based on conventional TS theory, both branches in Scheme 6 are energetically feasible. In recent years, the scope of ketone hydrogenation chemistry involving H₂ has been expanded with the discovery of catalysts in which the ligand proton donor site is not directly attached to the metal.^{64,65} The theoretical study by Yang mentioned above has supported a mechanism closely matching the one involving ruthenium alkoxide in Scheme 6, with hydride transfer to the ketone and base-assisted H₂ cleavage being central to the catalytic cycle.⁶² Thus, the qualitative symmetry arguments, the indication that *trans*-dihydride complexes related to 7-HRu-NH are powerful hydride donors, and the possibility of direct Ru–OR bond formation and its potential to cleave H₂ as discussed in the present work may have implications to ketone hydrogenation catalyzed by both metal–amine and non-metal–amine transition-metal catalysts.

■ ASSOCIATED CONTENT

■ Supporting Information

Absolute energies and Cartesian coordinates for the species in the figures. This material is available free of charge via the Internet at <http://pubs.acs.org>.

■ AUTHOR INFORMATION

Corresponding Author

*E-mail: fh19@aub.edu.lb.

Notes

The authors declare no competing financial interest.

■ ACKNOWLEDGMENTS

F.H. thanks the Arab Fund for a Distinguished Scholar Fellowship, TAMU-Qatar for computer time, and the University of Toronto for invited professorship. R.H.M. thanks the Natural Sciences and Engineering Research Council of Canada for a Discovery Grant.

■ REFERENCES

- (1) (a) Noyori, R.; Hashiguchi, S. *Acc. Chem. Res.* **1997**, *30*, 97. (b) Noyori, R.; Ohkuma, T. *Angew. Chem., Int. Ed.* **2001**, *40*, 40. (c) Noyori, R. *Angew. Chem., Int. Ed.* **2002**, *41*, 2008. (d) Jessop, P. G.; Ikariya, T.; Noyori, R. *Chem. Rev.* **1995**, *95*, 259.
- (2) (a) Clapham, S. E.; Hadzovic, A.; Morris, R. H. *Coord. Chem. Rev.* **2004**, *248*, 2201. (b) Samec, J. S. M.; Samec, J. S.; Backvall, J.-E.; Andersson, P. G. *Chem. Soc. Rev.* **2006**, *35*, 237. (c) Ikariya, T.; Blacker, A. J. *Acc. Chem. Res.* **2007**, *40*, 1300. (d) Dobereiner, G. E.; Crabtree, R. H. *Chem. Rev.* **2010**, *110*, 681.
- (3) (a) Saudan, L. A.; Saudan, C. N.; Debieux, C.; Wyss, P. *Angew. Chem., Int. Ed.* **2007**, *46*, 7473. (b) O, W. W. N.; Lough, A. J.; Morris, R. H. *Chem. Commun.* **2010**, *46*, 8240. (c) Ito, M.; Ootsuka, T.; Watari, R.; Shiibashi, A.; Himizu, A.; Ikariya, T. *J. Am. Chem. Soc.* **2011**, *133*, 4240.
- (4) (a) Doucet, H.; Ohkuma, T.; Murata, K.; Yokozawa, T.; Kozawa, M.; Katayama, E.; England, A. F.; Ikariya, T.; Noyori, R. *Angew. Chem., Int. Ed.* **1998**, *37*, 1703. (b) Takehara, J.; Hashiguchi, S.; Fujii, A.; Inoue, S.; Ikariya, T.; Noyori, R. *Chem. Commun.* **1996**, 233. (c) Kenny, J. A.; Versluis, K.; Heck, A. J. R.; Walsgrove, T.; Wills, M. *Chem. Soc. Chem. Commun.* **2000**, 99.
- (5) Abdur-Rashid, K.; Fatz, M.; Lough, A. J.; Morris, R. H. *J. Am. Chem. Soc.* **2001**, *123*, 7473.
- (6) (a) Abdur-Rashid, K.; Clapham, S. E.; Hadzovic, A.; Harvey, J. N.; Lough, A. J.; Morris, R. H. *J. Am. Chem. Soc.* **2002**, *124*, 15104. (b) Zimmer-De Iulius, M.; Morris, R. H. *J. Am. Chem. Soc.* **2009**, *131*, 11263.
- (7) Hadzovic, A.; Song, D.; MacLaughlin, C. M.; Morris, R. H. *Organometallics* **2007**, *26*, 5987.
- (8) Haack, K.-J.; Hashiguchi, S.; Fuji, A.; Ikariya, T.; Noyori, R. *Angew. Chem., Int. Ed. Engl.* **1997**, *36*, 285.
- (9) Maire, P.; Buttner, T.; Breher, F.; Le Floch, P.; Grützmacher, H. *Angew. Chem., Int. Ed.* **2005**, *44*, 6318.
- (10) (a) Hamilton, R. J.; Leong, C. G.; Bigam, G.; Miskolzie, M.; Bergens, S. H. *J. Am. Chem. Soc.* **2005**, *127*, 4152. (b) Hamilton, R. J.; Bergens, S. H. *J. Am. Chem. Soc.* **2006**, *128*, 13700.
- (11) Hamilton, R. J.; Bergens, S. H. *J. Am. Chem. Soc.* **2008**, *130*, 11979.
- (12) Takebayashi, S.; Bergens, S. H. *Organometallics* **2009**, *28*, 2349.
- (13) Baratta, W.; Chelucci, G.; Gladiali, S.; Siega, K.; Toniutti, M.; Zanette, M.; Zangrando, E.; Rigo, P. *Angew. Chem., Int. Ed.* **2005**, *44*, 6214.
- (14) Takebayashi, S.; Dabral, N.; Miskolzie, M.; Bergens, S. H. *J. Am. Chem. Soc.* **2011**, *133*, 9666.
- (15) Yamakawa, M.; Ito, H.; Noyori, R. *J. Am. Chem. Soc.* **2000**, *122*, 1466.
- (16) Noyori, R.; Yamakawa, M.; Hashiguchi, S. *J. Org. Chem.* **2001**, *66*, 7931.
- (17) (a) Brandt, P.; Roth, P.; Andersson, P. G. *J. Org. Chem.* **2004**, *69*, 4885. (b) Alonso, D. A.; Brandt, P.; Nordin, S. J. M.; Andersson, P. G. *J. Am. Chem. Soc.* **1999**, *121*, 9580.
- (18) (a) Petra, D. G. I.; Reek, J. N. H.; Handgraaf, J. W.; Meijer, E. J.; Dierkes, P.; Kamer, P. C. J.; Brussee, J.; Schoemaker, H. E.; van Leeuwen, P. W. N. M. *Chem.—Eur. J.* **2000**, *6*, 2818. (b) Handgraaf, J.-W.; Reek, J. N. H.; Meijer, E. J. *Organometallics* **2003**, *22*, 3150.
- (19) (a) Di Tommaso, D.; French, S. A.; Zanotti-Gerosa, A.; Hancock, F.; Palin, E. J.; Catlow, C. R. A. *Inorg. Chem.* **2008**, *47*, 2674. (b) Chen, H.-Y. T.; Di Tommaso, D.; Hogarth, G.; Catlow, C. R. A. *Dalton Trans.* **2011**, *40*, 402. (c) Chen, H.-Y. T.; Di Tommaso, D.; Hogarth, G.; Catlow, R. A. *Dalton Trans.* **2012**, *41*, 1867.
- (20) (a) Zhang, H.; Chen, D.; Zhang, Y.; Zhang, G.; Liu, J. *Dalton Trans.* **2010**, *39*, 1972. (b) Leyssens, T.; Peeters, D.; Harvey, J. N. *Organometallics* **2008**, *27*, 1514. (c) Vaclavik, J.; Kuzma, M.; Prech, P.; Kacer, P. *Organometallics* **2011**, *30*, 4822. (d) Bi, S.; Xie, Q.; Zhao, X.; Zhao, Y.; Kong, X. *J. Organomet. Chem.* **2008**, *693*, 633. (e) Puchta, R.; Dahlenburg, L.; Clark, T. *Chem.—Eur. J.* **2008**, *14*, 8898. (f) Li, H. X.; Lu, G.; Jiang, J. L.; Huang, F.; Wang, Z. X. *Organometallics* **2011**, *30*, 2349.
- (21) (a) Chen, Y.; Tang, Y.; Liu, S.; Lei, M.; Fang, W. *Organometallics* **2009**, *28*, 2078. (b) Chen, Y.; Tang, Y. H.; Lei, M. *Dalton Trans.* **2009**, 2359. (c) Chen, Z.; Chen, Y.; Tang, Y.; Liu, S.; Lei, M. *Dalton Trans.* **2010**, *39*, 2036. (d) Xin Zhang, X.; Guo, X.; Chen, Y.; Tang, Y.; Lei, M.; Fang, W. *Phys. Chem. Chem. Phys.* **2012**, *14*, 6003.
- (22) Chen, Y.; Liu, S.; Lei, M. *J. Phys. Chem. C* **2008**, *112*, 13524.
- (23) (a) Bertoli, M.; Choualeb, A.; Gusev, D. G.; Lough, A. J.; Moore, B. *Dalton Trans.* **2011**, *40*, 8941. (b) Bertoli, M.; Choualeb, A.; Lough, A. I.; Major, Q.; Moore, B.; Spasyuk, D.; Gusev, D. G. *Organometallics* **2011**, *30*, 3479.
- (24) Frisch, M. J.; et al. *Gaussian 09*, revision A.02; Gaussian, Inc.: Wallingford, CT, 2009.
- (25) Zhao, Y.; Truhlar, D. G. *Theor. Chem. Acc.* **2008**, *120*, 215.
- (26) (a) Tomasi, J.; Persico, M. *Chem. Rev.* **1994**, *94*, 2027. (b) Cossi, M.; Scalmani, G.; Rega, N.; Barone, V. *J. Chem. Phys.* **2002**, *117*, 43.
- (27) (a) McLean, A. D.; Chandler, G. S. *J. Chem. Phys.* **1980**, *72*, 5639. (b) Raghavachari, K.; Binkley, J. S.; Seeger, R.; Pople, J. A. *J. Chem. Phys.* **1980**, *72*, 650. (c) Rassolov, V. A.; Ratner, M. A.; Pople, J. A.; Redfern, P. C.; Curtiss, L. A. *J. Comput. Chem.* **2001**, *22*, 976.
- (28) Hay, P. J.; Wadt, W. R. *J. Chem. Phys.* **1985**, *82*, 279.
- (29) Höllwarth, A.; Böhlert, A. W.; Bohme, M.; Dapprich, S.; Gobbi, A.; Hollwarth, A.; Jonas, V.; Köhler, K. F.; Stegmann, R.; Veldkamp, A.; Frenking, G. *Chem. Phys. Lett.* **1993**, *208*, 111.
- (30) See: <https://bse.pnl.gov/bse/portal>.
- (31) Hehre, J.; Radom, L.; Schleyer, P. v. R.; Pople, J. A. *Ab Initio Molecular Orbital Theory*; Wiley: New York, 1986.
- (32) For a recent study with ample references pertaining to this problem, see: Li, H.; Wang, X.; Huang, F.; Lu, G.; Jiang, J.; Wang, Z.-X. *Organometallics* **2011**, *30*, 5233.

- (33) (a) Fryzuk, M. D.; MacNeil, P. A. *Organometallics* **1983**, *2*, 682. (b) Werner, H.; Hohn, A.; Dziallas, M. *Angew. Chem., Int. Ed. Engl.* **1986**, *25*, 1090. (c) Lunder, D. M.; Lobkovsky, E. B.; Streib, W. E.; Caulton, K. G. *J. Am. Chem. Soc.* **1991**, *113*, 1837. (d) Hauger, B. E.; Gusev, D.; Caulton, K. G. *J. Am. Chem. Soc.* **1994**, *116*, 208.
- (34) (a) Chin, B.; Lough, A. L.; Morris, R. H.; Schweitzer, C. T.; D'Agostino, C. *Inorg. Chem.* **1994**, *33*, 6278. (b) Wang, K.; Emge, T. G.; Goldman, A. S.; Li, C.; Nolan, S. P. *Organometallics* **1995**, *14*, 4929. (c) Goikhman, R.; Milstein, D. *Angew. Chem., Int. Ed.* **2001**, *40*, 1119.
- (35) (a) Rachidi, I. E.-I.; Eisenstein, O.; Jean, Y. *New J. Chem.* **1990**, *14*, 671. (b) Riehl, J. F.; Jean, Y.; Eisenstein, O.; Pelissier, M. *Organometallics* **1992**, *11*, 729.
- (36) Cotton, A. F. *Chemical Applications of Group Theory*, 3rd ed.; Wiley: New York, 1990.
- (37) Bersuker, I. *Chem. Rev.* **2001**, *101*, 1067.
- (38) Our initial attempts to use the CASSCF method, as implemented in *Gaussian09*, to minimize the two states for five-coordinate Ru=N considered in the present study encountered wave function and geometry convergence problems and were not pursued further. The origin of the problem appears to follow from a change of the composition of the atomic orbitals in the active space during minimization as the order of the two electronic states is altered when the geometry is changed, which we could not control because of lack of symmetry.
- (39) Haynes, A.; Meijer, A. J. H. M.; Lyons, J. R.; Adams, H. *Inorg. Chem.* **2009**, *48*, 28.
- (40) Hasanayn, F.; Abu-El-Ez, D. *Inorg. Chem.* **2010**, *49*, 9162.
- (41) Hasanayn, F.; Achord, P.; Braunstein, P.; Magnier, H. J.; Krogh-Jespersen, K.; Goldman, S. *Organometallics* **2012**, *31*, 4680.
- (42) (a) Abu-Hasanayn, F.; Cheong, P.; Oliff, M. *Angew. Chem.* **2002**, *41*, 2120. (b) Hasanayn, F.; Markarian, M.-Z.; Al-Rifai, R. *Inorg. Chem.* **2004**, *43*, 3691.
- (43) Jensen, V.; Poli, R. *J. Phys. Chem. A* **2003**, *107*, 1424.
- (44) Hoffmann, R.; Woodward, R. B. *Science* **1970**, *167*, 825.
- (45) A scan of the PES as a function of two equal Ru-H bond distances from 1.8 to 3.0 Å reveals a smooth increase in the energy as H₂ is brought closer to 7-Ru=N.
- (46) In ref 7, the alcohol adduct of a model of the ruthenium pyridyl amide **5** in Scheme 3 was calculated to be that of the square-pyramidal state of Ru=N. This shows that the alcohol adducts of the two states are of similar energy and their calculated energy order can be easily switched with small modifications in the complex or the computational level.
- (47) The calculations on the Binap alkoxide complex were carried out using the 6-31G(d,p) basis set.
- (48) Clapham, S. E.; Guo, R.; Zimmer-De Iulius, M.; Rasool, N.; Lough, A.; Morris, R. H. *Organometallics* **2006**, *25*, 5477.
- (49) Burn, M. J.; Fickes, M. G.; Hollander, F. J.; Bergman, R. G. *Organometallics* **1995**, *14*, 137.
- (50) Baratta, W.; Siega, K.; Rigo, P. *Chem.—Eur. J.* **2007**, *13*, 7479.
- (51) (a) Blum, O.; Milstein, D. *J. Am. Chem. Soc.* **1995**, *117*, 4582. (b) Blum, O.; Milstein, D. *J. Organomet. Chem.* **2000**, 593–594, 479.
- (52) Ritter, J. C. M.; Bergman, R. G. *J. Am. Chem. Soc.* **1998**, *120*, 6826.
- (53) Montag, M.; Zhang, J.; Milstein, D. *J. Am. Chem. Soc.* **2012**, *134*, 10328.
- (54) Sandoval, C. A.; Ohkuma, T.; Muñoz, K.; Noyori, R. *J. Am. Chem. Soc.* **2003**, *125*, 13490.
- (55) (a) Ito, M.; Hirakawa, M.; Murata, K.; Ikariya, T. *Organometallics* **2001**, *20*, 379. (b) Hartmann, R.; Chen, P. *Angew. Chem., Int. Ed.* **2001**, *40*, 3581. (c) Baratta, W.; Siega, K.; Rigo, P. *Chem.—Eur. J.* **2007**, *13*, 7479.
- (56) Casey, C. P.; Johnson, J. B.; Singer, S. W.; Cui, Q. *J. Am. Chem. Soc.* **2005**, *127*, 3100.
- (57) Friedrich, A.; Drees, M.; Schmedt auf der Gunne, J. S.; Schneider, S. *J. Am. Chem. Soc.* **2009**, *131*, 17552.
- (58) Hedberg, C.; Kallstrom, K.; Arvidsson, P. I.; Brandt, P.; Andersson, P. G. *J. Am. Chem. Soc.* **2005**, *127*, 15083.
- (59) O, W. W. N.; Lough, A. J.; Morris, R. H. *Organometallics* **2012**, *31*, 2137.
- (60) Lin, Z.; Marks, T. J. *J. Am. Chem. Soc.* **1987**, *109*, 7979.
- (61) Fulmer, G. R.; Herndon, A. N.; Kaminsky, W.; Kemp, R. A.; Goldberg, K. I. *J. Am. Chem. Soc.* **2011**, *133*, 17713.
- (62) Yang, X. *Inorg. Chem.* **2011**, *50*, 12836.
- (63) Handgraaf, J.-W.; Meijer, E. J. *J. Am. Chem. Soc.* **2007**, *129*, 3099.
- (64) (a) Kirchner, K. A.; Bauer, G. *Angew. Chem., Int. Ed.* **2011**, *50*, 5798. (b) Gunanathan, C.; Milstein, D. *Acc. Chem. Res.* **2011**, *44*, 588.
- (65) (a) Casey, C. P.; Bikzhanova, G. A.; Cui, Q.; Guzei, I. A. *J. Am. Chem. Soc.* **2005**, *127*, 14062. (b) Sui-Seng, C.; Freutel, F.; Lough, A. J.; Morris, R. H. *Angew. Chem., Int. Ed.* **2008**, *47*, 940.